White Rose Research Online

eprints@whiterose.ac.uk
https://eprints.whiterose.ac.uk
Universities of Leeds, Sheffield and York

Deposited via The University of Sheffield.

White Rose Research Online URL for this paper:
https://eprints.whiterose.ac.uk/id/eprint/158161/

Version: Accepted Version

Article:
Ezeh, O.H. and Susmel, L. (2020) On the notch fatigue strength of additively manufactured polylactide (PLA). International Journal of Fatigue, 136. 105583. ISSN: 0142-1123

https://doi.org/10.1016/j.ijfatigue.2020.105583

Article available under the terms of the CC-BY-NC-ND licence (https://creativecommons.org/licenses/by-nc-nd/4.0/).

Reuse
This article is distributed under the terms of the Creative Commons Attribution-NonCommercial-NoDerivs (CC BY-NC-ND) licence. This licence only allows you to download this work and share it with others as long as you credit the authors, but you can't change the article in any way or use it commercially. More information and the full terms of the licence here: https://creativecommons.org/licenses/

Takedown
If you consider content in White Rose Research Online to be in breach of UK law, please notify us by emailing eprints@whiterose.ac.uk including the URL of the record and the reason for the withdrawal request.

UNIVERSITY OF LEEDS
University of Sheffield
UNIVERSITY of York

On the Notch Fatigue strength of additively manufactured polylactide (PLA)

O. H. Ezeh and L. Susmel
Department of Civil and Structural Engineering, The University of Sheffield, Mappin Street, Sheffield, S1 3JD, United Kingdom

Corresponding Author: Prof. Luca Susmel
Department of Civil and Structural Engineering
The University of Sheffield, Mappin Street, Sheffield, S1 3JD, UK
Telephone: +44 (0) 114 222 5073
Fax: +44 (0) 114 222 5700
E-mail: l.susmel@sheffield.ac.uk

ABSTRACT

The strength and cracking behaviour under fatigue loading of additively manufactured polylactide (PLA) was investigated experimentally to quantify and model the role of notches. These tests were run under load ratios equal to -1 and to 0. Being supported by the experimental evidence, 3D-printed PLA was treated as a linear-elastic, isotropic, and homogenous material. This allowed the use of the Theory of Critical Distances to be extended also to the fatigue assessment of notched 3D-printed PLA. This theory was seen to return accurate estimates. This confirms that it can be used also to estimate fatigue lifetime of notched 3D-printed polymers.

Keywords: Additive manufacturing, PLA, notch, fatigue, critical distance.

Nomenclature

F_{max}, F_{min}	maximum and minimum force in the cycle
k	negative inverse slope
E	Young's modulus
L_M	critical distance in the medium-cycle fatigue regime
N_f	number of cycles to failure
N_{Ref}	reference number of cycles to failure ($N_{Ref}=2{\cdot}10^6$ cycles to failure)
Oxyz	local system of coordinates
P_S	probability of survival
R	load ratio ($R=\sigma_{min}/\sigma_{max}=F_{min}/F_{max}$)
T_σ	scatter ratio of the endurance limit for 90% and 10% probabilities of survival
θ, r	polar system of coordinates
θ_p	manufacturing angle
σ_{max}, σ_{min}	maximum and minimum stress in the cycle
$\sigma_{n,a}$	amplitude of the nominal net stress
$\sigma_{n,MAX-50\%}$	maximum value of the nominal net endurance limit at N_{Ref} cycles to failure for $P_S=50\%$
$\sigma_{n,A-50\%}$	amplitude of the nominal net endurance limit at N_{Ref} cycles to failure for $P_S=50\%$
$\sigma_{y,max}$	maximum value of the local linear-elastic stress parallel to axis y
σ_{MAX}	maximum value of the endurance limit at N_{Ref} cycles to failure
$\sigma_{MAX,50\%}$	maximum value of the endurance limit at N_{Ref} cycles to failure for $P_S=50\%$
$\sigma_{MAX,Design}$	maximum value of the design endurance limit at N_{Ref} cycles to failure for $P_S>90\%$
σ_{UTS}	ultimate tensile strength

1. Introduction

Polymers can be additively manufactured (AM) from powder, wires and flat sheets, with the material being melted and deposited using different techniques. Acrylonitrile butadiene styrene and polylactide (PLA) are among the most common polymers which can be 3D-printed at a relatively low cost by using off-the-shelf 3D-printers. AM polymers are used in situations of industrial interest to fabricate a variety of components such as, for instance, jigs, fixtures, high-precision gauges for quality control, custom car parts, and biomedical devices.

PLA is a polyester that is made from renewable sources such as sugar cane, starch and corn. As a result, PLA not only is biodegradable, but can also be recycled very easily.

The most common and cost-effective technology for 3D printing PLA is usually referred to as Fused Deposition Modelling (FDM). The FDM fabrication technology works by extruding plastic filaments through a heated nozzle. Initially, these filaments are deposited directly onto a platform (called "build plate") to create a first layer of material with the wanted shape. As this thin layer of material cools and hardens, it adheres to the build plate itself. After completing the very first layer, the build plate is lowered and the extrusion nozzle starts building the second layer of material. This is done by extruding plastic filaments that bind not only to each other, but also to the layer beneath them. Once this second layer is completed, the build plate is lowered again so that a new layer of plastic can be built. This additive process allow computer-aided design to be used to fabricate objects layer by layer, where the layer being build binds directly to the previous layer of material. In this context, it is important to mention that commercial FDM-printers usually manufacture the different layers by first creating the so-called shell. Shells are nothing but perimetric retaining walls that are used not only to contain the bulk material, but also to obtain a higher level of precision in terms of dimensions and shape.

Turning to the mechanical response of FDM-AM PLA, examination of the state of the art demonstrates that its behaviour under both static [1-6] and fatigue loading [7-10] is affected by a number of technological variables that include, amongst others: thickness of layers and shells, infill density, filling pattern, infill speed, diameter and temperature of the nozzle, printing direction, feed rate, printing speed, and temperature of the build plate. Although PLA is a plastic polymer, its mechanical response in the AM form is predominantly brittle, where the little level of ductility that is observed before final breakage varies as the printing direction changes [4, 5].

These considerations should make it evident that the mechanical and fatigue behaviour of AM PLA is rather complex. Fortunately, the complexity associated with the design problem can be reduced markedly by observing that, as long as objects are FDM-manufactured flat on the build plate, the effect of the printing direction can be disregarded, with this simplifying assumption resulting just in a little loss of accuracy [5, 10]. Therefore, in engineering situations of practical interest, the static and fatigue assessment of AM PLA can be performed by modelling it as a linear-elastic, homogenous and isotropic material [5, 6, 10].

As far as fatigue assessment is concerned, the design problem can be simplified even more by observing that the maximum stress in the cycle, σ_{max}, allows the effect of non-zero mean stresses to be taken into account in a simple, but accurate way [10, 11].

According to the above simplifying hypotheses based on the experimental evidence, if the effect of the raster angle is neglected and the load cycles are modelled in terms of σ_{max}, the fatigue assessment can then be performed by directly using the unifying scatter band plotted in the SN chart of Fig. 1 [10, 11]. This scatter band was built by post processing a large number of experimental results that were generated by testing AM PLA fabricated by making the printing direction vary in the range 0°-90°. Further these un-notched specimens with different material lay-ups (obtained by changing the raster angle) were tested by setting the load ratio, $R=\sigma_{min}/\sigma_{max}$, equal to -1, -0.5, 0, and 0.3. In the SN diagram of Fig. 1 σ_{UTS} is the material ultimate tensile strength, N_f is the number of cycles to failure, k is the negative inverse slope, P_S is the probability of survival, $\sigma_{MAX,50\%}$ is the maximum value of the endurance limit extrapolated at $N_{Ref}=2\cdot10^6$ cycles to failure, and T_σ is the scatter ratio of the endurance limit for 90% and 10% probabilities of survival.

As per the SN diagram of Fig. 1, whenever it is not possible to determine experimentally the fatigue strength of the specific AM PLA being employed, then the fatigue assessment is recommended to be performed (for $P_S>90\%$) by adopting a design curve having negative inverse slope, k, equal to 5.5 and endurance limit, $\sigma_{MAX,Design}$, at $N_{Ref}=2\cdot10^6$ cycles to failure equal to $0.1\cdot\sigma_{UTS}$ [10, 11].

One of the most important features of AM is that this technology allows the fabrication of objects having very intricate geometries. In this context, since AM components can contain complex geometrical features, their static/fatigue strength is obviously affected by localised stress/strain concentration phenomena.

As far as notches are concerned, examination of the state of the art demonstrates that the Theory of Critical Distances (TCD) [12-14] is the most powerful candidate to be used to design AM components against fatigue loading. The TCD groups together a number of design methods that all make use of a material length scale parameter to assess the extent of damage. Further, the local stress-fields needed to determine the TCD design stresses are calculated by adopting a simple linear-elastic constitutive law, with this holding true also in the presence of non-linear stress-strain responses [12]. Such unique features make the TCD appropriate for being used by directly post-processing the results from conventional linear-elastic Finite Element (FE) analyses.

As far as static loading is concerned, it has already been demonstrated that the TCD is successful in predicting the strength of notched AM PLA [5, 6]. In contrast, so far the TCD has never been attempted to be used to estimate fatigue lifetime of components of AM PLA containing notches of different sharpness. Filling this knowledge gap represents the ultimate goal of the theoretical/experimental work being summarised and discussed in what follows.

2. Experimental details

The notched specimens shown in Figs 2a, 2b, and 2c were FDM-manufactured by using commercial 3D-printer Ultimaker 2 Extended+. The parent material used for the present experimental investigation was white New Verbatim PLA with density equal to 1.24 g/cm^3, glass transition temperature to 58 °C, tensile yield stress to 63 MPa and tensile elongation to 4%. The wires of this polymer had initial diameter equal to 2.85 mm and were extruded through a brass nozzle down to a diameter equal to 0.4 mm. All the notched samples were manufactured flat on the build-plate (Fig. 2d). As recommended by the manufacturer of the FDM-printer being used, the specimens were fabricated by setting the temperature of the nozzle equal to 240°C, the build-plate temperature to 60°C, the print speed to 30mm/s, the shell thickness equal to 0.4 mm (see Fig. 3a), and the layer height to 0.1 mm. It is important to point out here also that the specimens were fabricated by setting the infill density equal to 100%, with this resulting in a void fraction invariably equal to zero. The average mechanical properties of the PLA FDM-manufactured according to this procedure were as follows [5]: Young's modulus equal to 3479 MPa, 0.2% proof stress equal to 41.7 MPa and ultimate tensile strength, σ_{UTS}, equal to 42.9 MPa.

In its standard configuration, 3D-printer Ultimaker 2 Extended+ deposits the filaments always at ±45° to the principal printing axis (Fig. 2d). Therefore, to investigate the existing interactions between raster direction and notch fatigue strength, the tested specimens were FDM-fabricated by setting the manufacturing angle, θ_p, equal to 0°, 30°, and 45°. According to Fig. 2d, θ_p was defined as the angle between the sample's longitudinal axis and the principal manufacturing direction. This simple stratagem allowed us to manufacture specimens having a ±45° lay-up (θ_p=0°), a -15°/+75° lay-up (θ_p=30°) and, finally, a 0°/+90° lay-up (θ_p=45°).

To better clarify the role of the shell in 3D-printed objects, Fig. 3a shows three different examples of specimens manufactured by setting the shell thickness equal to 0 mm, 0.4 mm and to 0.8 mm. This figure shows that the samples manufactured with no shell at all were characterised by very rough lateral surfaces. In contrast, setting the shell thickness equal to either 0.4 mm or 0.8 mm allowed specimens with very smooth lateral surfaces to be fabricated [5]. Further, by carefully observing these pictures it is possible to see the printed filaments being at 45° to the specimen vertical axis, with these samples being fabricated by setting angle θ_p equal to 0°.

Finally, for the sake of completeness, the stress vs. strain curves generated experimentally by testing plain specimens manufactured by setting θ_p equal to 0°, 30°, 45°, 60° and 90° are shown in Fig. 3b [5].

The geometries and nominal dimensions of the notched specimens that were tested in the Structures Laboratory of the University of Sheffield are shown in Figs 2a to 2c. The actual dimensions of the manufactured specimens were measured systematically by using a high precision calliper and an optical microscope. This methodical check of the specimens' dimensions made it evident that the 3D-printer being used was capable of additively manufacturing objects of PLA by consistently reaching an adequate level of accuracy. In particular, the obtained tolerances were seen to be in the range ±0.2 mm.

The sharply notched specimens (Fig. 2c) were manufactured by setting in the CAD solid model the opening angle equal to 35° and the notch root radius equal to 0 mm. This was done in order to manufacture specimens containing stress raisers that were as sharp as possible. The systematic measurements taken using an optical microscope revealed that the actual average value of the notch root radius was equal to 0.15±0.05 mm.

The fatigue tests were run by using an electric fatigue table that was specifically developed for this experimental investigation. As shown in Fig. 2e, the notched specimens were tested under sinusoidal axial loading, with the magnitude of the applied axial force being gathered continuously during testing through an axial loading cell. In parallel, the nominal vertical displacement of the shaking plate was monitored by using a linear LVDT. Since the net cross-sectional area of the specimens was very small (i.e., 6 mm x 3 mm), the fatigue tests were run up to the complete breakage of the samples themselves. All the experiments were run at a frequency of 10 Hz. The nominal load ratio, $R=F_{min}/F_{max}$, was set not only equal to -1, but also to 0, where the zero-tension configuration was used to investigate the effect of superimposed static stresses on the overall fatigue strength of notched 3D-printed PLA. The run-out tests were all stopped at $2 \cdot 10^6$ cycles to failure. All the tests were run at room temperature. The latter aspect is very important because, due to its polymeric nature, the fatigue behaviour of 3D-printed PLA is expected to be highly sensitive to temperature. This testing procedure was developed in accordance with the pertinent standard recommendations [15-17].

Finally, the number of notched samples that were tested for any experimental configuration being investigated are listed in Tab. 1.

3. Cracking behaviour in the presence of notches

The cracking behaviour of the notched specimens being tested was investigated by using a simple optical microscope. The direct inspection of the fracture surfaces allowed us to study the crack initiation phase in the vicinity of the notch tips as well as the subsequent crack propagation process.

The matrix of failures seen in Fig. 4 reports some representative examples of the crack paths that were observed not only as the sharpness of the tested notch increased, but also for different values of the manufacturing angle, θ_p, and the load ratio, R.

As per the fracture surfaces shown in Fig. 4, the fatigue cracks were seen to initiate, in the notch tip regions, always on material planes that were perpendicular to the direction of the applied loading. Accordingly, the hypothesis can be formed that the process resulting in the initiation of the fatigue cracks was governed by a Mode I-driven failure mechanism, with this process resulting in embryonic cracks having length approaching 0.4 mm (i.e., having length approximately equal to the shell thickness). Such an opening-mode governed initiation phase was observed in the majority of the notched specimens being tested, with this holding true independently of notch sharpness, raster angle, and load ratio. However, in some cases, the cracks were seen to initiate slightly away from the apices of the stress raisers, with the initial growth occurring at the interface between the shell used to delimit the notch tip and the bulk material.

Turning to the subsequent propagation phase, the cracks grew along irregular paths that followed mainly the orientation of the extruded filaments (Fig. 4). Thus, as observed also in the absence of stress gradients [10], the assumption can be made that, independently of notch sharpness, material lay-up, and load ratio, the final breakage of the notched samples was the result of the following simultaneous failure mechanisms: (i) de-bonding between adjacent filaments, (ii) de-bonding between adjacent layers and (iii) rectilinear cracking of the filaments themselves.

4. Notch Fatigue Strength

The results generated according to the experimental protocol described in the previous section are summarised in the SN charts reported in Fig. 5 for the sharp notches (Fig. 2c), in Fig. 6 for intermediate notches (Fig. 2b), and in Fig. 7 for the blunt notches (Fig. 2a). These standard log-log fatigue diagrams were built by plotting the amplitude of the nominal net stress, $\sigma_{n,a}$, against the number of cycles to failure, N_f. The scatter bands shown in the above charts refer to a probability of survival, P_S, equal to 90% and 10%. They were calculated, with a confidence level of 95%, by assuming a log-normal distribution of the number of cycles to failure for each stress level [18-20]. For the purpose of clarity, the results from the statistical re-analyses are summarised also in Tab. 1 in terms of negative inverse slope, k, endurance limit, $\sigma_{n,A\text{-}50\%}$, referred to the nominal net area and extrapolated, for P_S=50%, at $N_{Ref}=2\cdot10^6$ cycles to failure, and, finally, scatter ratio, T_σ, of the endurance limit for 90% and 10% probabilities of survival.

The same statistical procedure was used also to determine the scatter bands that are reported in the SN charts of Fig. 8. In these diagrams all the results generated for any type of notch are plotted together in terms of maximum value of the nominal net stress, $\sigma_{n,max}$.

The Wöhler diagrams shown in Figs 5 to 7 together with Tab. 1 make it evident that, likewise conventional engineering materials, the fatigue strength of notched AM PLA tends to slightly increase as the load ratio, $R=F_{min}/F_{max}$, increases from -1 to 0. Further, for a given notch/raster angle configuration, the value of the negative inverse slope, k, slightly increases as the mean stress increases. Lastly, similar to what is observed in un-notched specimens [7-11], Figs 5 to 7 and Tab. 1 confirm that the raster angle somehow affects the overall fatigue behaviour of AM PLA also in the presence of stress concentration phenomena, although it has to be said that this effect appears to be very little.

As done with plain AM PLA [10, 11], an attempt was then made to simplify the problem under investigation by post-processing the generated experimental results in terms of maximum value of the nominal net stress, $\sigma_{n,max}$. This simple assumption takes as a starting point the idea that the maximum stress in the cycle can be used to model the mean stress effect in fatigue since, by definition, its magnitude also depends on the mean value - in fact, $\sigma_{n,max}=\sigma_{n,m}+\sigma_{n,a}$. As mentioned earlier, the results from this re-analysis are summarised in the SN diagrams of Fig. 8.

According to the charts seen in Fig. 8, initially it can be pointed out that, for a given value of the load ratio, the effect of manufacturing angle θ_p appears to be negligible, with this engineering assumption resulting just in a little loss of accuracy. As to this simplification, it can be said that, compared to what is observed in un-notched specimens [10, 11], the presence of stress concentration phenomena tends to mitigate the effect of the raster angle even more markedly. Therefore, based on this experimental evidence, the engineering hypothesis can be formed that, as long as objects are manufactured flat on the build plate, notched AM PLA can be treated as a homogenous and isotropic material - i.e., its mechanical behaviour can be model accurately without taking into account the effect of the material lay-up explicitly.

Turning back to the effect of non-zero mean stresses, the SN diagrams of Fig. 8 make it evident that, in terms of maximum stress in the cycle, the fatigue strength under R=0 appears to be slightly higher than the corresponding fatigue strength under R=-1. However, the relatively low values for ratio T_σ (see Fig. 8) strongly support the idea that the influence of superimposed static stresses can be modelled effectively by simply using the maximum stress in the cycle. This engineering assumption is expected to result just in a little loss of design accuracy that can be in any case compensated via the use of adequate safety factors.

The outcomes from the post-processing of the experimental results as discussed in the present section will be used in what follows to re-formulate the Theory of Critical Distances (TCD) [12] to make it suitable for performing also the fatigue assessment of notched AM PLA.

5. The Theory of Critical Distances

As long as objects of PLA are additively manufactured flat on the build plate, the mechanical behaviour displayed by the 3D-printed polymer under investigation allows the following simplifying assumptions to be made:

- the effect of the raster angle can be neglected so that AM PLA can be assumed to behave like a homogenous and isotropic material;
- the stress vs. strain response of AM PLA can be modelled by adopting a simple linear-elastic constitutive law (Fig. 3b) [5];
- the effect of superimposed static stresses on the fatigue behaviour of AM PLA can directly be taken into account via the maximum stress in the cycle.

Based on these simplifying engineering hypotheses, an attempt can then be made to use the TCD also to assess the fatigue strength of notched AM PLA. The fundamentals of the TCD used in the form of the Point, Line and Area Method will briefly be reviewed in what follows, with this powerful design theory being directly reformulated in terms of maximum stress in the cycle. In particular, according to the fatigue behaviour observed in plain AM PLA [10, 11], the mean stress effect will be attempted to be taken into account directly via the maximum stress also in the presence of notches.

The TCD was first devised by Neuber [21] and Peterson [22] back in the 1940s-50s in the form of the Line Method and the Point Method, respectively. From a philosophical point of view, this theory postulates that fatigue damage in the presence of stress concentrators is assessed via an effective stress whose magnitude depends on: (i) the entire linear-elastic stress field acting on the material in the vicinity of the crack initiation locations; (ii) a length scale parameter which represents the underlying material microstructure [12-14]. In more detail, the material critical distance is assumed to define the size of the process zone, where the process zone represents that portion of material controlling the overall strength of the component being designed [14, 23]. Further, the TCD intrinsic material distance is seen to be somehow related also to the size of the dominant source of microstructural heterogeneity [24].

The formalisations of the TCD proposed by Neuber [21] and Peterson [22] were originally devised to perform the fatigue assessment in the high-cycle fatigue regime. In other words, these

approaches were formalised so that they could be used to estimate fatigue/endurance limits of metallic components containing geometrical features of all kinds.

In 2007 Susmel and Taylor [25] reformulated the TCD to make it suitable for estimating fatigue damage also in the finite lifetime regime. This advanced version of the TCD was developed based on the hypothesis that the material length scale parameter needed to determine the required effective stress decreases as the number of cycles to failure increases, i.e. [25, 26]:

$$L_M(N_f) = A \cdot N_f^B \tag{1}$$

In definition (1), A and B are material constants that can be determined by running a series of standard fatigue experiments. It is worth recalling here that, for a given material, constants A and B are seen to vary with the load ratio. In contrast, their values do not change as profile and sharpness of the notch being designed change [25, 26]. The procedure to be followed to determine constants A and B in power law (1) will be reviewed in detail at the end of the present section.

As soon as the L_M vs. N_f relationship is known from the experiments, the TCD can be used in different forms, where the alternative formalisations of this theory can directly be derived by simply changing size and shape of the integration domain used to calculate the effective stress.

In more detail, if the TCD is applied in the form of Peterson's Point Method, then the maximum value of the effective stress can directly be determined as follows (see Figs 9a and 9b) [27, 28]:

$$\sigma_{eff,max} = \sigma_{y,max}\left(\theta = 0°, r = \frac{L(N_f)}{2}\right) \tag{2}$$

Alternatively, according to Neuber's Line Method, the maximum value of the effective stress has to be determined by averaging the maximum value of the linear-elastic stress, $\sigma_{y,max}$, along a line over a distance equal to $2L_M(N_f)$, i.e. (Fig. 9c) [28]:

$$\sigma_{eff,max} = \frac{1}{2 \cdot L_M(N_f)} \int_0^{2 \cdot L_M(N_f)} \sigma_{y,max}(\theta = 0°, r) \cdot dr \tag{3}$$

Finally, as per Sheppard's intuition [29], the maximum value of the effective stress can also be determined by averaging the maximum value of the 1st principal stress over a semicircle with radius equal to $L_M(N_f)$ and centred at the notch apex [12, 28]. In other words, effective stress $\sigma_{eff,max}$ determined according to the so-called Area Method takes on the following value (Fig. 9d):

$$\sigma_{eff,max} = \frac{4}{\pi L_M^2(N_f)} \int_0^{\frac{\pi}{2}} \int_0^{L_M(N_f)} \sigma_{1,max}(\theta, r) \cdot r \cdot dr \cdot d\theta \quad (4)$$

In this context, it is worth mentioning that there is also a three-dimensional formalisation of the TCD which is known as the Volume Method [12]. This form of the TCD postulates that the effective stress has be calculated by averaging the linear-elastic maximum principal stress over a hemisphere having radius equal to $1.54 \cdot L_M(N_f)$ and centred at the notch apex [30].

Having determined $\sigma_{eff,max}$ according to one of the strategies reviewed above, the number of cycles to failure can then be estimated directly from the SN curve quantifying the fatigue strength of the un-notched material being designed, i.e. [25]:

$$N_f = N_{Ref} \cdot \left(\frac{\sigma_{MAX}}{\sigma_{eff,max}} \right)^k \quad (5)$$

In relationship (5) σ_{MAX} is the plain material endurance limit extrapolated at N_{Ref} cycles to failure and k is the negative inverse slope.

Ed. (1) together with definitions (2), (3), and (4) make it evident that fatigue lifetime of notched components can be estimated according to the TCD provided that suitable recursive numerical procedures are used [25]. This is an obvious consequence of the fact that while N_f is the unknown variable in the design problem, it is needed to estimate also the critical distance value from Eq. (1). However, as discussed in Refs [25, 26], this is a trivial problem that can be solved by using simple and standard optimisation algorithms.

Turning to the calibration of the L_M vs. N_f relationship, according to definition (1), in theory, two different pieces of experimental information should be enough to estimate fatigue constants A and B. For instance, they could directly be derived from the critical distance determined under static loading and the critical distance estimated in the high-cycle fatigue regime (see Ref. [25] for a detailed description of this possible strategy to estimate constants A and B). Unfortunately, this approach is not at all straight forward to be used in practice for the following two reasons [14, 25]: (i) because the stress based approach is not accurate enough when it comes to model the behaviour of materials failing in the low-cycle fatigue regime; (ii) because the position of the knee point defining the endurance limit in the high-cycle fatigue regime is seen to vary as profile and sharpness of the calibration notches being tested vary.

These two limitations can be overcome by simply determining constants A and B in Eq. (1) from the un-notched material fatigue curve and from another fatigue curve determined by testing specimens containing a notch having known profile and known sharpness [25, 26]. This way of

estimating constants A and B is explained through the SN diagram shown in Fig. 9e. In particular, according to the Point Method's *modus operandi*, given a reference number of cycles to failure, N_f^*, it is straightforward to determine the distance from the notch tip, $L_M(N_f)/2$, at which the maximum value of the linear-elastic stress, $\sigma_{y,max}$, equals the value of the maximum stress that has to be applied to the plain material to break it at N_f^* cycles to failure (Fig. 9e). According to this simple procedure, the critical distance value can then be determined for all the N_f values from the low- to the high-cycle fatigue regime, allowing constants A and B to be determined unambiguously [25, 26].

This simple strategy will be used in the next section to check whether the linear-elastic TCD is successful also in estimating fatigue lifetime of notched AM PLA.

6. Validation by experimental data

In order to apply the TCD to post-process the notch fatigue results summarised in the charts of Figs 5 to 7, local stresses were determined using commercial FE software ANSYS®. The relevant linear-elastic stress fields in the notched specimens shown in Figs 2a to 2c were determined by solving bi-dimensional FE models built by using 4-node structural plane elements (plane 182). According to the hypotheses formed in the previous section, the numerical solutions were calculated by assuming that the AM polymer under investigation behaves like a linear-elastic, homogeneous and isotropic material. Finally, in order to determine the required stress fields by systematically reaching an adequate level of numerical accuracy, the mesh density in the vicinity of the notch tips was gradually increased until convergence occurred.

According to the calibration strategy summarised in Fig. 9e, constant A and B in Eq. (1) for the AM PLA being assessed were determined from the following two fatigue curves:

- the experimental plain fatigue curve derived in Ref. [10] for P_S equal to 50% (Fig. 1);
- the fatigue curve (Fig. 8a) determined by post-processing all the results generated by testing the sharply notched specimens (Fig. 2c).

Considering that the average value of σ_{UTS} for the AM polymer under investigation was equal to 42.9 MPa [5], according to the scatter band seen in Fig. 1 the plain material fatigue constants were estimated to be as follows: $\sigma_{MAX,50\%}$=6.7 MPa at $N_{Ref}=2\cdot10^6$ cycles to failure and k=5.1.

The fatigue curve generated by testing specimens containing notches with root radius, r_n, equal to 0.15 mm was used because, according to our previous experience with other materials [14, 25], to calibrate constants A and B it is always advisable to use stress raisers that are as sharp as possible.

By post-processing the local-linear elastic stress field determined numerically for the sharply notched specimens, the procedure sketched in Fig. 9e applied by using the two calibration fatigue curves mentioned above returned the following values for constants A and B:

$$L_M(N_f) = 16.4 \cdot N_f^{-0.242} \text{ [mm]} \quad (6)$$

This L_M vs. N_f relationship was then used to post-process the experimental results being generated according to both the Point and the Area Method. Unfortunately, the Line Method could not be used because the length of the required integration domain in the medium/low-cycle fatigue regime - i.e., $2L(N_f)$ - was larger than half net-width of the specimens [12].

The SN diagrams of Fig. 10 that plot the normalised maximum value of the effective stress, $\sigma_{eff,max}/\sigma_{UTS}$, vs. the number of cycles to failure, N_f, confirm that the systematic use of the TCD returned estimates mainly falling within the plain material scatter band. This result is certainly satisfactory since, from a statistical point of view, a predictive method cannot be more accurate than the experimental information used for its calibration.

It is worth concluding by observing that, in situations of practical interest, the fatigue assessment of notched components of AM PLA can then be performed accurately by using relationship (6) together with the unifying design curve proposed in Ref. [10] and having $\sigma_{MAX,Design}=0.1\cdot\sigma_{UTS}$ and k=5.5 (Fig. 1). By so doing, notched 3D-printed PLA can be designed against fatigue for a probability of survival, P_S, that is always larger than 90% even when specific calibration experiments cannot be run.

7. Conclusions

In the present investigation, a large number of specimens were tested to study the fatigue behaviour of AM PLA weakened by notches having different sharpness. The notched samples being tested in the Structures Laboratory of the University of Sheffield were all FDM-manufactured flat on the build plate. In order to assess the effect of the raster direction, these specimens were fabricated by setting manufacturing angle θ_p equal to 0°, 30, and 45° (Fig. 2). The specimens sketched in Figs 2a to 2c were tested under fully-reversed axial loading (R=-1) as well as under zero-tension (R=0). The accuracy of the TCD in estimating fatigue lifetime of notched components of AM PLA was checked against the fatigue results being generated.

According to the outcomes from this experimental/theoretical work, it is possible to draw the following conclusions that are strictly valid solely for objects of PLA 3D-printed flat on the build plate:

- in notched AM PLA the cracking behaviour under fatigue loading is governed by three predominant failure mechanisms, i.e. rectilinear cracking of the filaments, de-bonding between adjacent filaments, and de-bonding between adjacent layers;
- fatigue cracks grow along irregular paths that follow mainly the orientation of the extruded filaments;
- an increase of the notch sharpness is seen to result in a decrease of the fatigue strength;
- in the presence of stress concentration phenomena, the effect of the raster angle on the overall fatigue strength of AM PLA can be neglected with little loss of accuracy;
- the mean stress effect in notch fatigue of AM PLA can be effectively taken into account by addressing the design problem in terms of maximum stress in the cycle;
- the TCD is proven to be remarkably accurate also in assessing notch fatigue strength of 3D-printed PLA;
- if appropriate experiments cannot be run, notch fatigue strength of AM PLA can be assessed according to the TCD by using Eq. (6) together with a unifying design curve with k=5.5 and $\sigma_{MAX,Design}=0.1\cdot\sigma_{UTS}$ (at $2\cdot10^6$ cycles to failure for $P_S\geq90\%$).

References

[1] Lanzotti A, Grasso M, Staiano G, Martorelli M. The impact of process parameters on mechanical properties of parts fabricated in PLA with an open-source 3-D printer. Rapid Prototyping J 2015;21(5):604-617.

[2] Casavola C, Cazzato A, Moramarco V, Pappalettere C. Orthotropic mechanical properties of fused deposition modelling parts described by classical laminate theory. Mater Des 2016;90;453-458.

[3] Chacón JM, Caminero MA, García-Plaza E, Núñez PJ. Additive manufacturing of PLA structures using fused deposition modelling: Effect of process parameters on mechanical properties and their optimal selection. Mater Des 2017;124:143-157.

[4] Song Y, Li Y, Song W, Yee K, Lee K-Y, Tagarielli VL. Measurements of the mechanical response of unidirectional 3D-printed PLA. Mater Des 2017;123:2017:154-164.

[5] Ahmed AA, Susmel L. A material length scale based methodology to assess static strength of notched additively manufactured polylactide (PLA). Fatigue Fract Eng Mater Struct 2018;41(10):2071-2098.

[6] Ahmed AA, Susmel L. Static assessment of plain/notched polylactide (PLA) 3D-printed with different in-fill levels: equivalent homogenised material concept and Theory of Critical Distances. Fatigue Fract Eng Mater Struct. 2019;(42):883–904.

[7] Letcher T, Waytashek M. Material property testing of 3D-printed specimen in PLA on an entry-level 3D-printer. In: Proceedings of the ASME 2014 International Mechanical Engineering

Congress & Exposition (IMECE2014), 14-20 November 2014, Montreal, Quebec, Canada, IMECE2014-39379.

[8] Afrose F, Masood SH, Iovenitti P, Nikzad M, Sbarski I. Effects of part build orientations on fatigue behaviour of FDM-processed PLA material. Prog Addit Manuf 2016;1:21-28.

[9] Jerez-Mesa R, Travieso-Rodriguez JA, Llumà-Fuentes J, Gomez-Gras G, Puig D. Fatigue lifespan study of PLA parts obtained by additive manufacturing. Procedia Manufacturing 2017;13:872-879.

[10] Ezeh OH, Susmel L. Fatigue strength of additively manufactured polylactide (PLA): effect of raster angle and non-zero mean stresses. Int J Fatigue 2019;126:319-326.

[11] Ezeh OH, Susmel L. Reference strength values to design against static and fatigue loading polylactide additively manufactured with in-fill level equal to 100%. Mat Design Process Comm. 2019;e45. https://doi.org/10.1002/mdp2.45.

[12] Taylor D. The Theory of Critical Distances: A New Perspective in Fracture Mechanics. Elsevier Science, 2007.

[13] Susmel L. The Theory of Critical Distances: a review of its applications in fatigue. Eng Frac Mech 2008;75:1706-1724.

[14] Susmel L. Multiaxial notch fatigue: from nominal to local stress–strain quantities. Cambridge (UK): Woodhead & CRC; 2009.

[15] Anon. Standard Test Method for Uniaxial Fatigue Properties of Plastics. ASTM D7791; 2017.

[16] Anon. Standard Practice for Conducting Force Controlled Constant Amplitude Axial Fatigue Tests of Metallic Materials. ASTM E466; 2011.

[17] Anon. Japan Society of Mechanical Engineers, Standard method of statistical fatigue testing. JSME S 002-1981, 1981.

[18] Anon. Standard Practice for Statistical Analysis of Linear or Linearized Stress-Life (S-N) and Strain-Life (ε-N) Fatigue Data. ASTM E739; 2015.

[19] Spindel JE, Haibach E. Some considerations in the statistical determination of the shape of S-N cruves. In: Statistical Analysis of Fatigue Data, ASTM STP 744 (Edited by Little, R. E. and Ekvall, J. C.), pp. 89–113, 1981.

[20] Al Zamzami I, Susmel L. On the accuracy of nominal, structural, and local stress based approaches in designing aluminium welded joints against fatigue. Int J Fatigue 2017;101:137-158.

[21] Neuber H. Theory of notch stresses: principles for exact calculation of strength with reference to structural form and material. Springer Verlag, Berlin, II Ed. 1958.

[22] Peterson RE. Notch Sensitivity. In: Sines G., Waisman J. L., Editors. Metal Fatigue. New York. McGraw Hill 1959;293-306.

[23] Susmel L. A unifying approach to estimate the high-cycle fatigue strength of notched components subjected to both uniaxial and multiaxial cyclic loadings. Fatigue Fract Engng Mater Struct. 2004;27:391-411.

[24] Taylor D. The Theory of Critical Distances: A link to micromechanisms. Theor Appl Fract Mec 2017;90:228–233.

[25] Susmel L. Taylor, D., A novel formulation of the Theory of Critical Distances to estimate Lifetime of Notched Components in the Medium-Cycle Fatigue Regime. Fatigue Fract Eng Mater Struct 2007;30(7):567-581.

[26] Susmel L, Taylor D. The Theory of Critical Distances to estimate lifetime of notched components subjected to variable amplitude uniaxial fatigue loading. Int J Fatigue 2011;33:900-911.

[27] Tanaka K. Engineering formulae for fatigue strength reduction due to crack-like notches. Int J Fracture 1983;22:R39-R45.

[28] Taylor D. Geometrical effects in fatigue: a unifying theoretical model. Int J Fatigue 1999;21:413-420.

[29] Sheppard SD. Field effects in fatigue crack initiation: long life fatigue strength. ASME J Mech Des 1991;113:188-194.

[30] Bellett D, Taylor D, Marco S, Mazzeo E, Guillois J, Pircher T. The fatigue behaviour of three-dimensional stress concentrations. Int J Fatigue 2005;27:207-221.

List of Captions

Table 1. Summary of the experimental results generated by testing the notched specimens of PLA shown in Figs 2a to 2c.

Figure 1. Unifying scatter band [10] suitable for designing additively manufactured PLA against fatigue – Data taken from Refs [7, 8, 10].

Figure 2. Geometries of the notched specimens being tested (a-c), definition of manufacturing angle θ_p (d), and overview of the testing set-up (e).

Figure 3. Examples of specimens manufactured with different values of the shell thickness (a); stress vs strain curves generated by testing the plain specimens under tensile loading (b) [5].

Figure 4. Cracking behaviour displayed by the tested notched AM PLA (in the pictures the specimen's longitudinal axis is vertical and the notch tip on the left-hand side).

Figure 5. SN curves determined by post-processing (in terms of stress amplitude) the results generated by testing the specimens containing the sharp notches.

Figure 6. SN curves determined by post-processing (in terms of stress amplitude) the results generated by testing the specimens containing the intermediate notches.

Figure 7. SN curves determined by post-processing (in terms of stress amplitude) the results generated by testing the specimens containing the blunt notches.

Figure 8. SN curves determined by post-processing the notch results in terms of maximum stress in the cycle.

Figure 9. Notched component subjected to fatigue loading (a); the TCD applied in the form of the Point (b), Line (c) and Area Method (d); calibration of the L_M vs. N_f relationship by using two different fatigue curves (e).

Figure 10. Accuracy of the TCD applied in the form of the Point and Area Method in estimating the fatigue lifetime of the notched specimens of AM PLA tested under axial fatigue loading.

Tables

Notch Type	θ_p *[°]*	N. of Samples	R	k	$\sigma_{n,A-50\%}$ *[MPa]*	T_σ
Blunt	45	13	-1	6.3	9.2	1.698
	45	8	0	8.3	7.5	1.520
	30	9	-1	4.8	6.7	1.299
	30	9	0	7.5	6.9	1.435
	0	10	-1	5.4	8.2	1.702
	0	9	0	7.3	7.3	1.335
Intermediate	45	9	-1	4.3	4.4	1.451
	45	9	0	5.0	4.3	1.442
	30	8	-1	4.8	5.1	1.305
	30	9	0	5.4	4.7	1.291
	0	10	-1	4.1	4.9	1.818
	0	7	0	4.6	4.4	1.252
Sharp	45	8	-1	3.7	4.1	1.170
	45	8	0	4.5	3.7	1.326
	30	8	-1	4.1	4.8	1.749
	30	7	0	4.7	3.9	1.265
	0	8	-1	3.7	4.3	1.477
	0	8	0	5.0	4.5	1.280

Table 1. Summary of the experimental results generated by testing the notched specimens of PLA shown in Figs 2a to 2c.

Figures

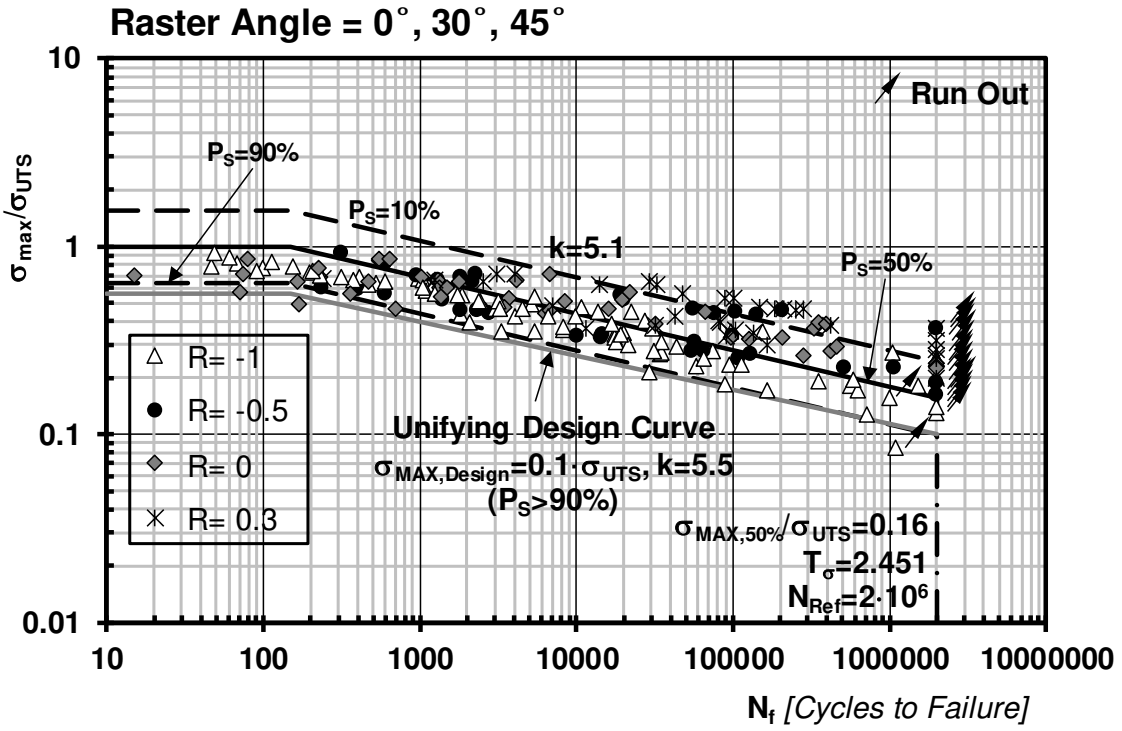

Figure 1. Unifying scatter band [10] suitable for designing additively manufactured PLA against fatigue – Data taken from Refs [7, 8, 10].

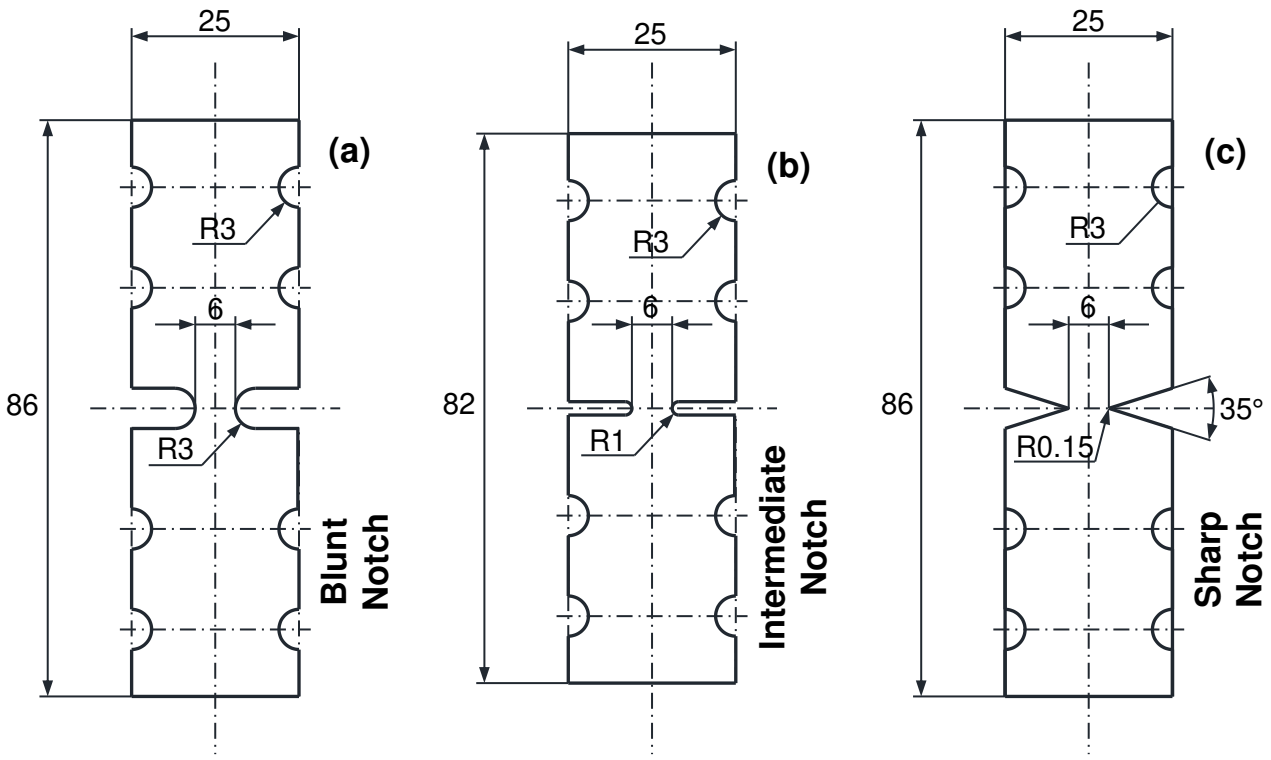

Thickness = 3 mm – Nominal dimensions in millimetres

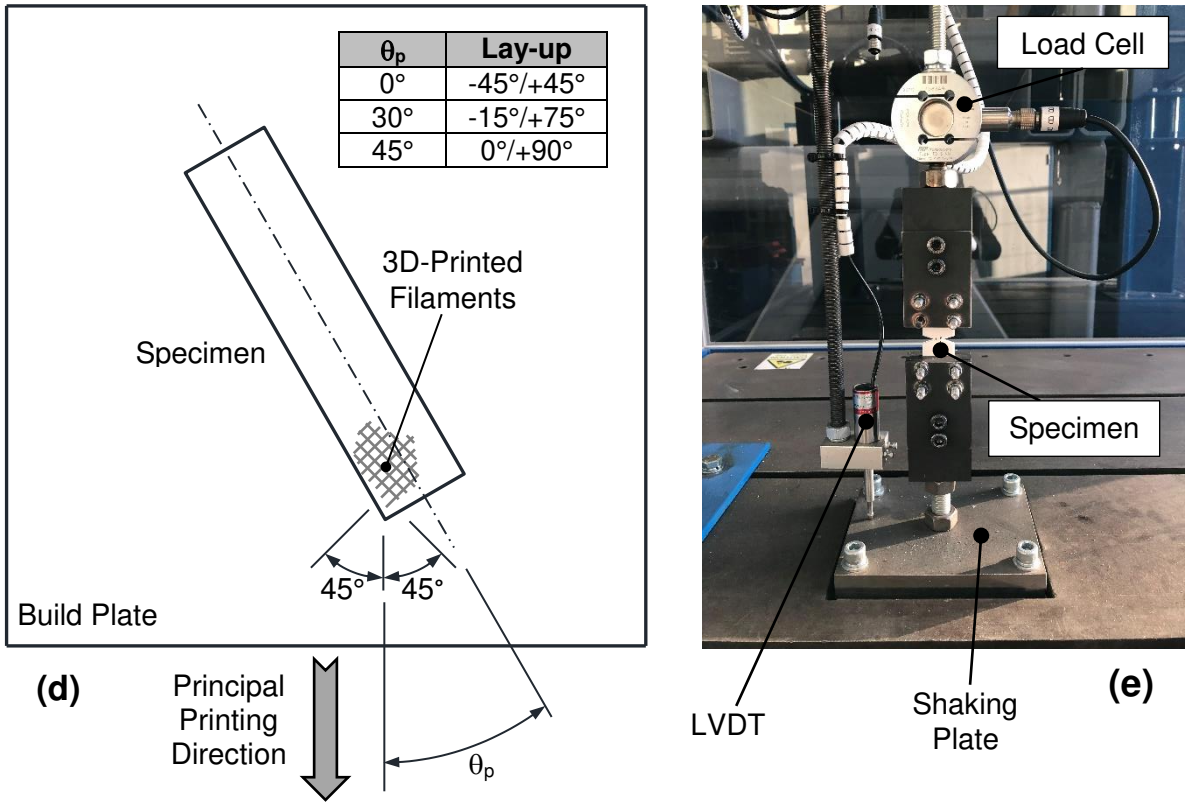

Figure 2. Geometries of the notched specimens being tested (a-c), definition of manufacturing angle θ_p (d), and overview of the testing set-up (e).

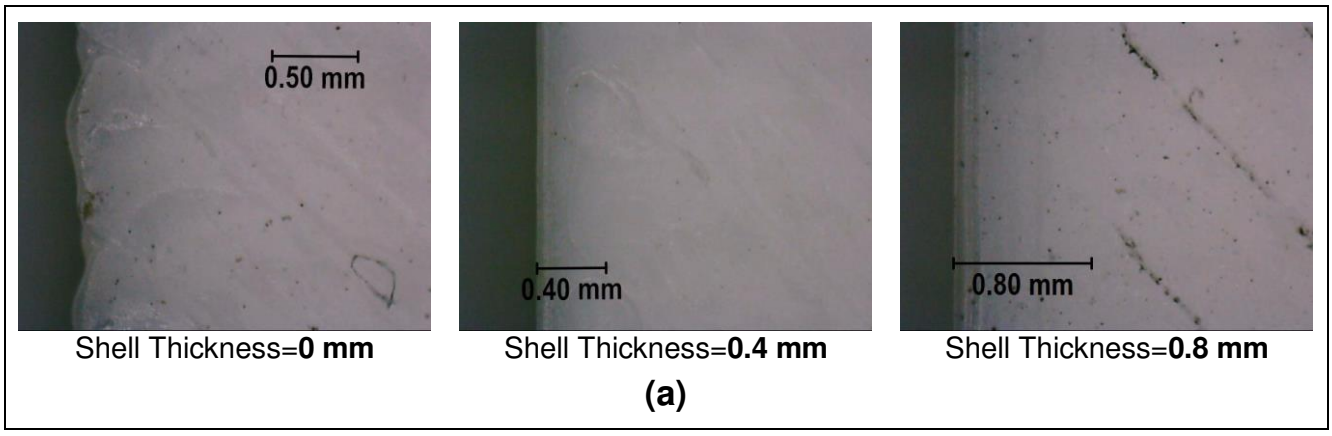

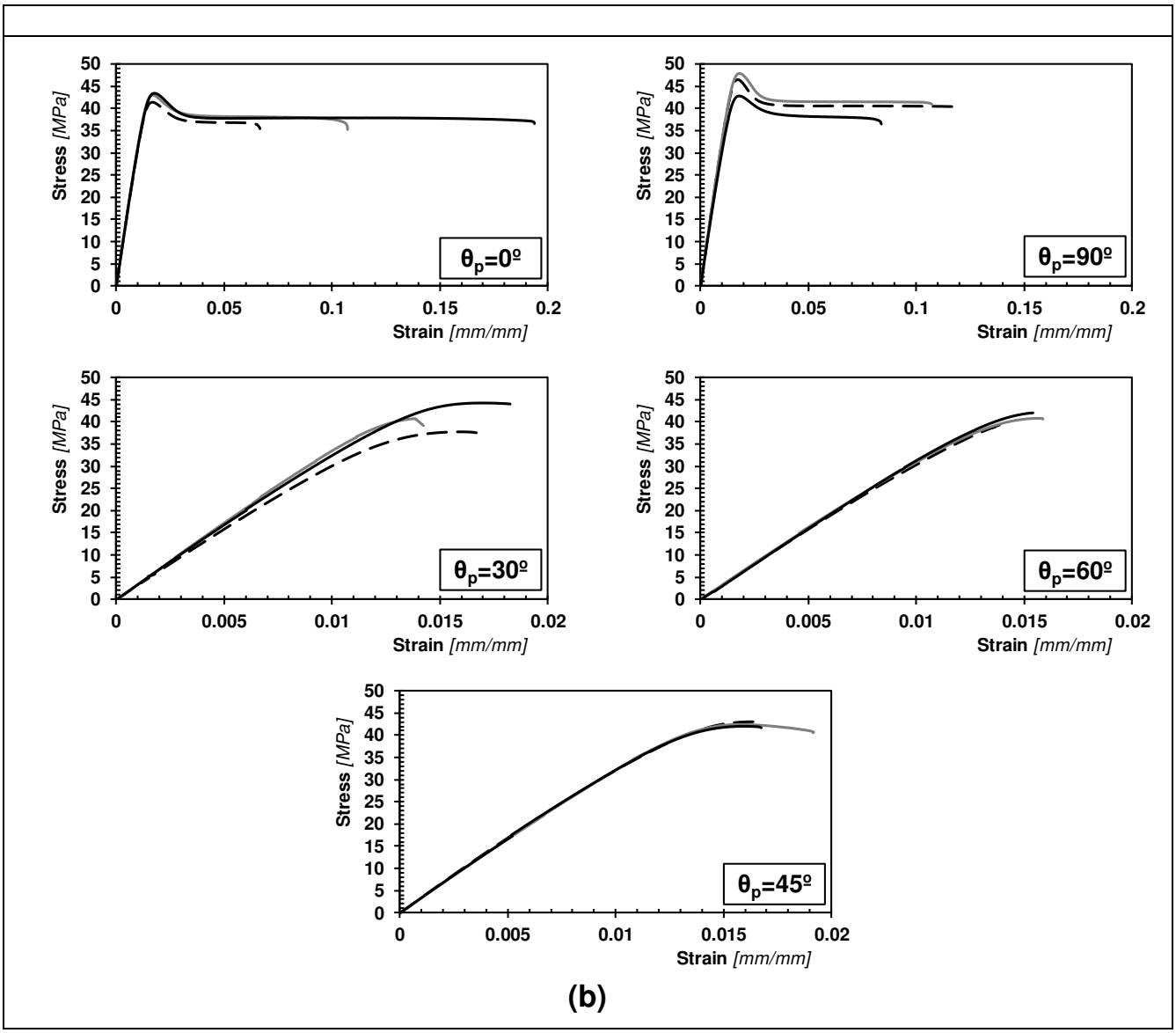

Figure 3. Examples of specimens manufactured with different values of the shell thickness (a); stress vs strain curves generated by testing the plain specimens under tensile loading (b) [5].

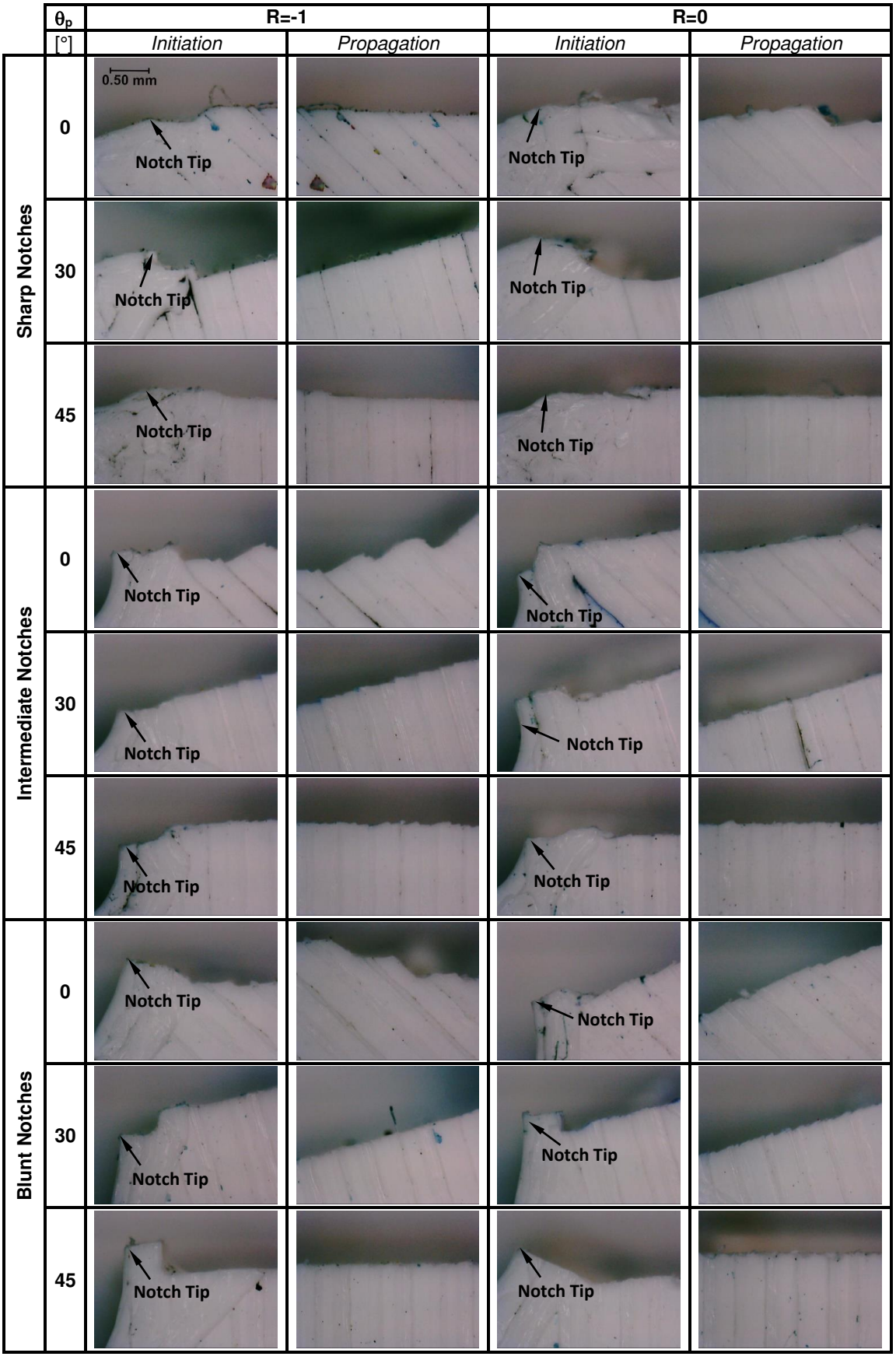

Figure 4. Cracking behaviour displayed by the tested notched AM PLA (in the pictures the specimen's longitudinal axis is vertical and the notch tip on the left-hand side).

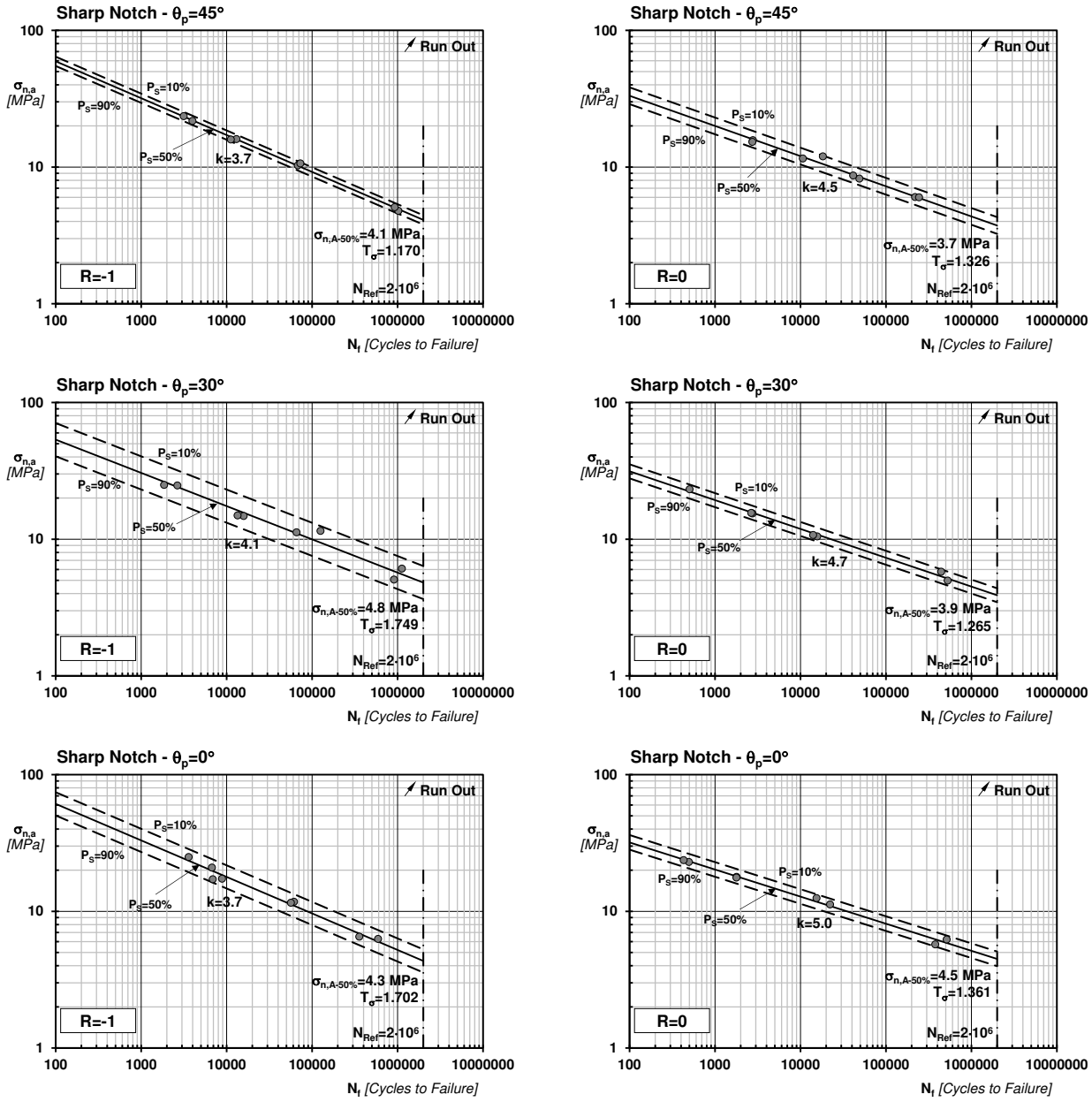

Figure 5. SN curves determined by post-processing (in terms of stress amplitude) the results generated by testing the specimens containing the sharp notches.

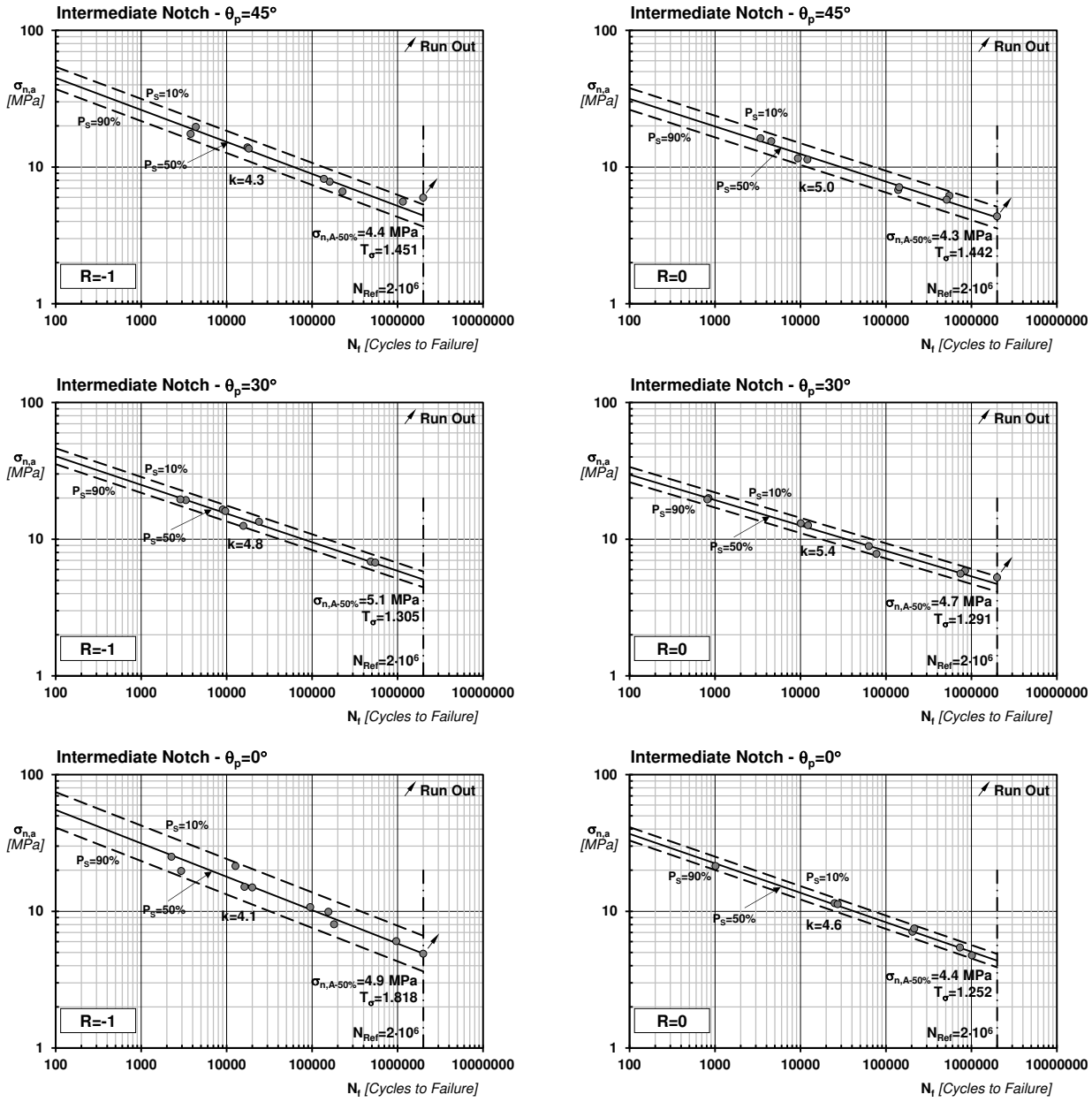

Figure 6. SN curves determined by post-processing (in terms of stress amplitude) the results generated by testing the specimens containing the intermediate notches.

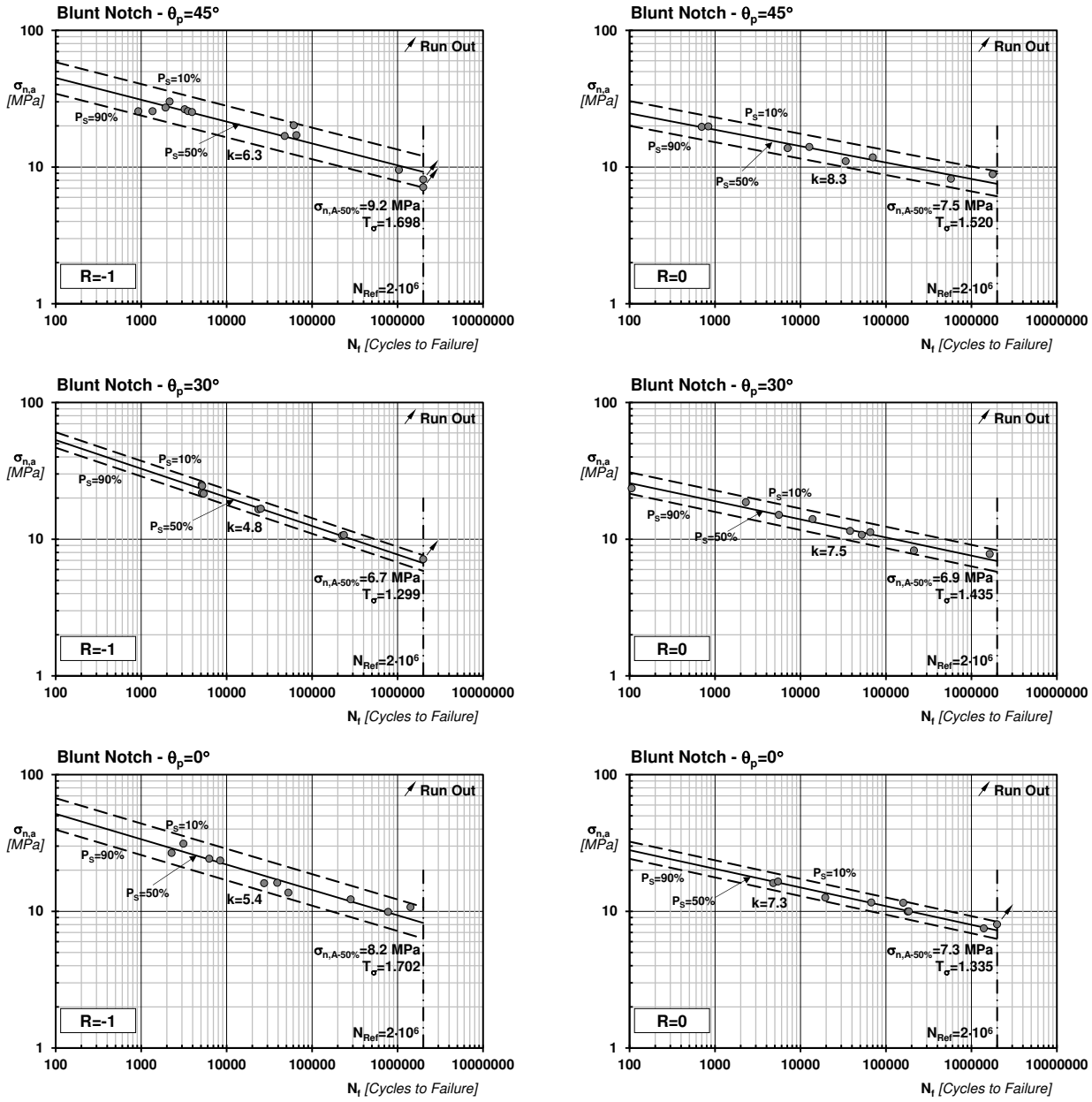

Figure 7. SN curves determined by post-processing (in terms of stress amplitude) the results generated by testing the specimens containing the blunt notches.

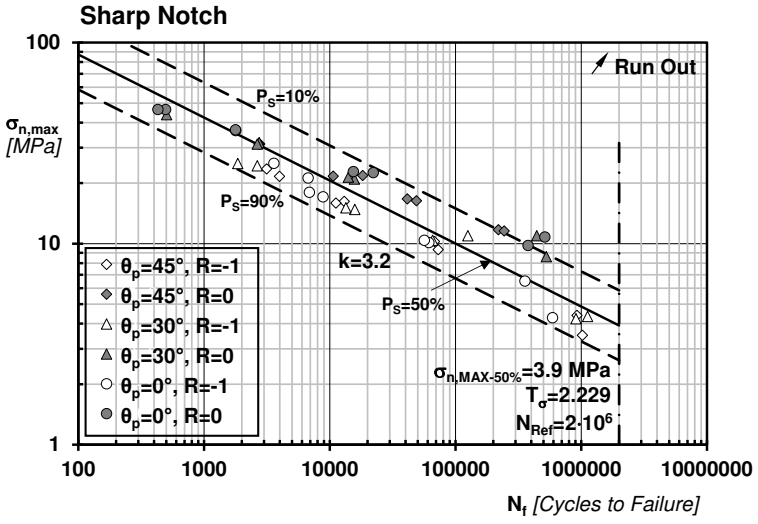

(a)

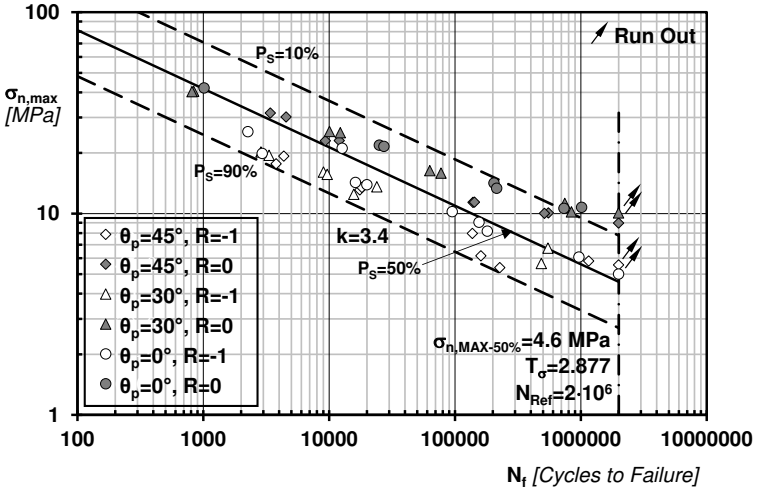

(b)

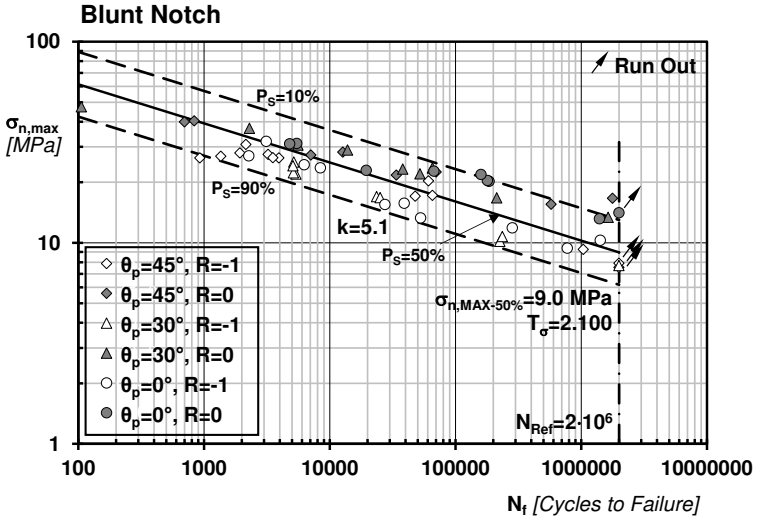

(c)

Figure 8 SN curves determined by post-processing the notch results in terms of maximum stress in the cycle.

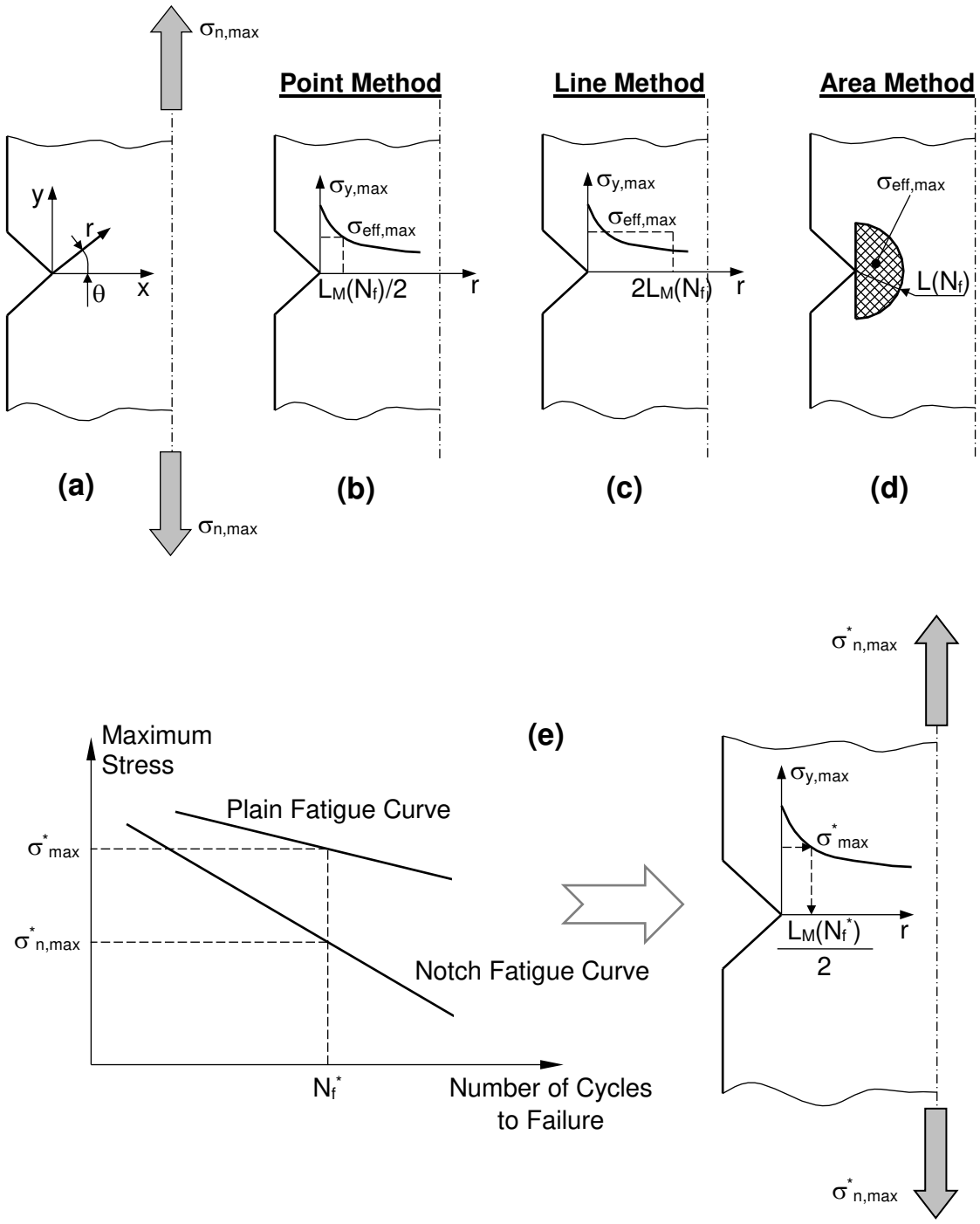

Figure 9. Notched component subjected to fatigue loading (a); the TCD applied in the form of the Point (b), Line (c) and Area Method (d); calibration of the L_M vs. N_f relationship by using two different fatigue curves (e).

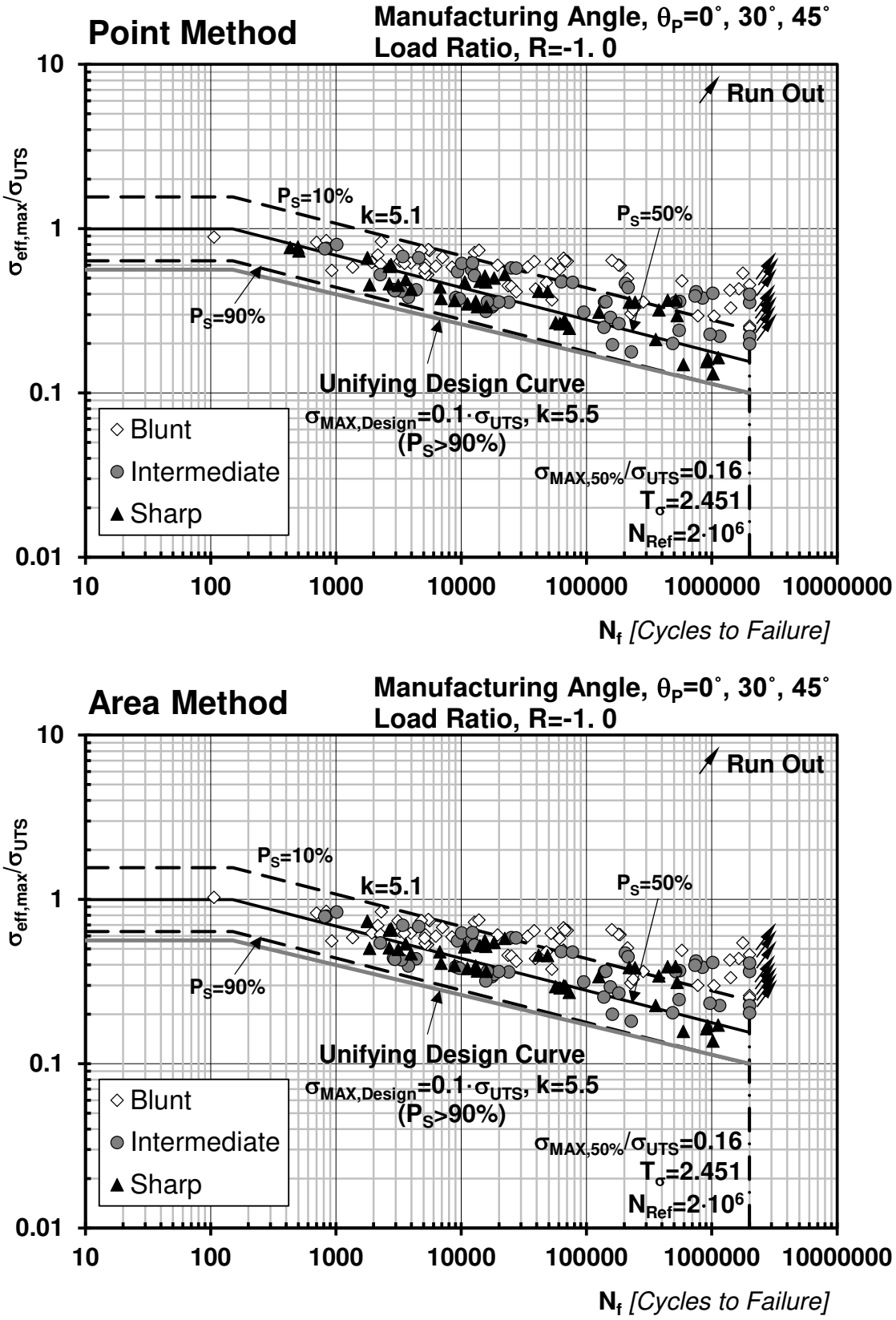

Figure 10. Accuracy of the TCD applied in the form of the Point and Area Method in estimating the fatigue lifetime of the notched specimens of AM PLA tested under axial fatigue loading.